

Highly Active Titania Photocatalyst Particles of Controlled Crystal Phase, Size, and Polyhedral Shapes

Fumiaki Amano · Taikei Yasumoto · Orlando Omar Prieto Mahaney · Satoshi Uchida · Tamaki Shibayama · Yoshihiro Terada · Bunsho Ohtani

Published online: 2 April 2010
© Springer Science+Business Media, LLC 2010

Abstract Mesoscopic crystalline anatase particles of titanium(IV) oxide (titania) with decahedral morphology and with octahedral morphology were synthesized by gas-phase reaction of titanium(IV) chloride with oxygen and hydrothermal reaction of titanate nanowires in an alkaline medium, respectively, and their photocatalytic activities in relation with their crystal morphology were investigated.

Keywords Anatase titania · Decahedral and octahedral particles · Photocatalytic activity · Crystalline facets

1 Introduction

Enhancement of the photocatalytic activity of anatase titanium(IV) oxide (titania) for decomposition of water and organic compounds [1, 2] has been a challenging subject.

F. Amano · B. Ohtani (✉)
Catalysis Research Center, Hokkaido University,
Sapporo 001-0021, Japan
e-mail: ohtani@cat.hokudai.ac.jp

F. Amano · T. Yasumoto · O. O. P. Mahaney · B. Ohtani
Graduate School of Environmental Science, Hokkaido
University, Sapporo 060-0810, Japan

S. Uchida · B. Ohtani
Research Center for Advanced Science and Technology, The
University of Tokyo, Tokyo 153-8904, Japan

T. Shibayama
Center for Advanced Research of Energy Conversion Materials,
Hokkaido University, Sapporo 060-8628, Japan

Y. Terada
Fujikura Ltd, Sakura, Chiba 285-8500, Japan

Extension of the absorption region from the original ultraviolet (UV) to visible range (VR) without reduction of photocatalytic activity in UV is one of the strategies for activity enhancement. Although there have been a number of trials for preparation of visible light-sensitive titania photocatalysts by, for example, doping of main-group elements [3, 4], loading gold nanoparticles [5, 6] and surface modification with transition-metal anions [7], their photocatalytic activity in the VR has been low and far from the level of practical applications. Another strategy for activity enhancement is to reduce recombination of photoexcited electron-positive hole pairs. Electron–hole pairs, which are generated by the band-gap excitation of titania, are transferred to surface-adsorbed reactants with competition of mutual recombination. Since recombination is expected to occur at grain boundaries and crystalline defects, the use of single-crystalline particles with a low density of defects is one strategy. In the present study, we prepared octahedral [8] and decahedral [9] single-crystalline anatase particles through a hydrothermal reaction and a gas-phase reaction, respectively, and confirmed their high level of photocatalytic activity in several photocatalytic reaction systems. The effect of crystal morphology, octahedral or decahedral, as a new parameter possibly governing photocatalytic activity, is discussed.

2 Experimental

2.1 Materials

Mesoscopic octahedral anatase titania particles (OAT) were prepared as follows [8]. A precursor, titanate nanowires, was prepared by hydrothermal reaction of titania particles (Degussa P25) suspended in a 17-mol L⁻¹

potassium hydroxide solution at 383 K for 20 h [10]. The thus-prepared nanowires (100 mg) were stirred in Milli-Q water (30 mL) and heated in a Teflon-lined autoclave (100 mL) at 443 K for 24 h to obtain OAT. Mesoscopic decahedral anatase titania particles (DAT) were prepared by a gas-phase reaction of titanium(IV) chloride ($TiCl_4$) and oxygen (O_2) with a rapid heating and quenching technique as reported previously [9] and briefly described as follows. The vapor of $TiCl_4$ liberated by bubbling of argon (200 $mL\ min^{-1}$) into $TiCl_4$ at 358 K was mixed with an O_2 stream (1,200 $mL\ min^{-1}$) and fed into a quartz glass tube (50 mm in outer diameter) rotated around the cylindrical axis at a speed of 55 rpm for homogeneous heating and heated from outside the quartz tube by an O_2 -hydrogen (H_2) flame burner. The resultant particles were collected in a corn-shaped glass-fiber filter, washed thoroughly with water to remove residual chlorine and dried under vacuum. Titania particles obtained commercial or supplied as reference titania catalysts by the Catalysis Society of Japan were used as received. Degussa P25 (P25) was a gift from Nippon Aerosil. Physical and structural properties of commercial and reference titania samples have been reported elsewhere [11].

2.2 Characterization

Titania samples were characterized by powder X-ray diffractometry (XRD; Rigaku RINT ULTIMA with $Cu\ K_\alpha$ radiation), scanning and scanning transmission electron microscopy (SEM; JEOL JSM-7400F and STEM; Hitachi HD-2000) and gas-adsorption measurement (Yuasa Ionics Autosorb 6AG surface area and pore size analyzer). Specific surface area (SSA) was estimated from nitrogen absorption at 77 K using the Brunauer–Emmett–Teller equation. Density of lattice defects was evaluated by the measurement of electron accumulation by photoirradiation under deaerated conditions in the presence of methanol as an electron donor (hole scavenger) by double-beam photoacoustic spectroscopy [11, 12]; photoacoustic signal was calibrated to absolute density of electron accumulation in the sample at 625 nm under photoexcitation at 365 nm. Zeta-potential measurements were performed using a Zetasizer Nano (Malvern) zeta-potential analyzer. A sample powder (20 mg) was suspended in an aqueous solution (40 mL) and pH of the suspension was adjusted by addition of diluted hydrochloric acid or an aqueous solution of sodium hydroxide. Amount of adsorption of silver ions (Ag^+) on the surface of particulate titania samples in the dark was estimated by measuring the decrease in Ag^+ concentration 2 h after addition of a 50-mg sample to aqueous silver sulfate solutions (25 $mmol\ L^{-1}$, 5 mL) using a Shimadzu AA-6200 flame atomic absorption spectrophotometer.

2.3 Photocatalytic Reactions

Photocatalytic activities were examined in several reaction systems: (1) dehydrogenation of methanol with in situ photodeposited platinum (from hexachloroplatinic acid), (2) oxidative decomposition of acetic acid or methanol in aerated aqueous suspensions and (3) deposition of silver from silver salt solutions using a 400-W high-pressure mercury arc as a light source. Details have been reported in supplementary material (ESI) of the previous report [8].

3 Results and Discussion

3.1 Crystal Morphology

Shape-controlled particles with octahedral and decahedral morphologies were obtained by hydrothermal reaction of titanate nanowires and gas-phase reaction of $TiCl_4$ and O_2 , respectively, as shown in Fig. 1. In their XRD patterns, negligible and only very small peaks of rutile were found as well as peaks assignable to anatase as a main component, respectively. The sizes of particles were in the mesoscopic range: ca. 30 and 150 nm. It has been confirmed by TEM analyses that each particle is of single crystal and that the eight facets in OAT are of equivalent {101} lattice planes [8], while DAT exposes eight trapezoidal {101} planes and two square {001} planes [9]. These lattice planes are schematically shown in Fig. 2.

It is well known that natural anatase crystals are often found in octahedral shape, since the {101} facets are thermodynamically most stable [13, 14]. Therefore the octahedral shape of anatase particles prepared by the hydrothermal reaction, which is expected to be similar to the conditions of production of natural minerals, might be controlled by thermodynamics to expose the most stable facets, while DAT, exposing also {001} facets in addition to {101} ones, might be produced under kinetically controlled conditions in which supply of a source material, $TiCl_4$, in the gaseous reaction may not be sufficient. The size of DAT was slightly larger than that of OAT, but study for controlling the size by more precise control of heating with an infrared furnace and of gas flow is now in progress [15].

3.2 Physical Properties of Polyhedral Particles

Physical properties of representative OAT and DAT used in photocatalytic activity tests, as well as those of P25 as a reference, are summarized in Table 1.

SSA of DAT was ca. one-fifth of those of OAT and P25, reflecting the marked difference in particle size as estimated from SEM images. Products of SSA in the unit of

Fig. 1 Scanning electron microscopic images of OAT (a, b) and DAT (c, d) anatase single-crystalline particles

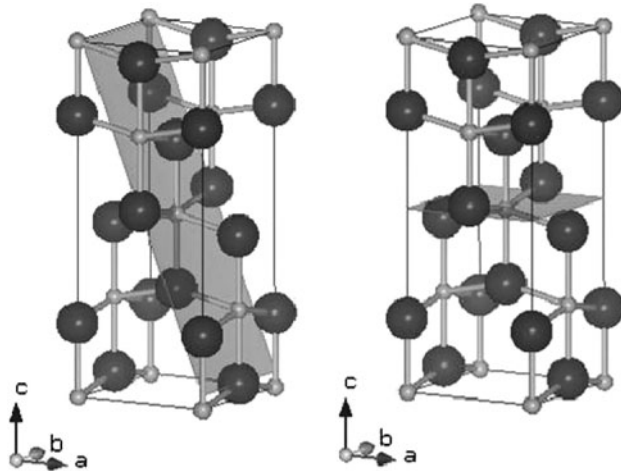
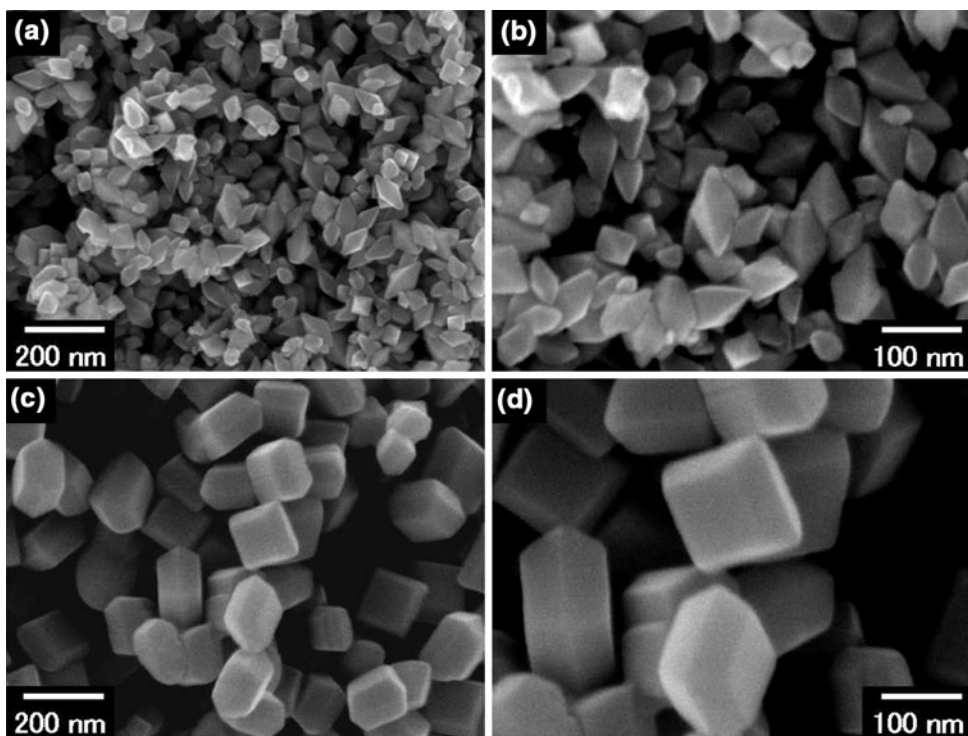


Fig. 2 Schematic presentation of (101) (left) and (001) (right) lattice planes in an anatase unit cell. Black and gray balls represent oxygen (O^{2-}) and titanium (Ti^{4+}) ions, respectively

$m^2 g^{-1}$ and particle size in the unit of nm were almost 1,500 for all samples. Thus, it is reasonable to assume that the particles uniform spherical particles with a density of ca. $4 g cm^{-3}$ and that the present polyhedral particles are not so different from ordinary titania samples.

Densities of defects in OAT and DAT showed slightly different tendencies; the density in OAT was almost two-times larger than that in P25 even though their SSAs were comparable, while the density of DAT was a little smaller than that of P25 in spite of the fact that SSA of DAT was ca. five times smaller than that of P25. As has been suggested in our previous report [16], the density may be the sum of densities of surface and bulk defects, the former of which increases with SSA and the latter of which is estimated to be in the range of $20\text{--}30 \mu\text{mol g}^{-1}$. On the basis of these considerations, DAT seems to have a comparable

Table 1 Physical properties of octahedral (OAT) and decahedral (DAT) single-crystalline anatase titania particles and a reference titania sample, Degussa P25

Sample	Specific surface area ($m^2 g^{-1}$)	Particle size ^a (nm)	Crystalline	Density of defects ($\mu\text{mol g}^{-1}$)	Ag^+ adsorption ($\mu\text{mol g}^{-1}$)
OAT	40	30	Anatase	108	390(10) ^d
DAT	9	150	Anatase (rutile) ^b	36	110(12) ^d
P25	48	30	Anatase, rutile ^c	50	480(10) ^d

^a Approximate average size estimated from SEM images

^b Anatase with a small amount of rutile

^c A mixture of anatase and rutile

^d Figures in parentheses show the amount of Ag^+ adsorption per unit surface area in the unit of $\mu\text{mol m}^{-2}$

surface density of defects, while OAT has relatively high density of surface or bulk defects despite the expectation that crystallinity of particles with controlled morphology is higher than that of ordinary particles. Possible reasons for the higher density of defects in OAT are (1) the exposed {101} facets essentially possess defects working as electron traps due to their reconstruction structure and (2) hydrothermal treatment, unlike high-temperature gas-phase reaction, produces defects on the surfaces. At present we have no evidence for any reasons. The effects of defects, as well as the amount of Ag^+ adsorption (Table 1), are also discussed in the following section.

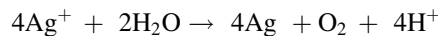
Figure 3 is plots of zeta potential as a function of pH of the suspension of OCT, DAT or P25 particles. The curves shifted upward, i.e., to the positive side, in that order. It is well known that there are hydroxyl groups on the surface of titania which are in equilibrium among $-\text{OH}_2^+$, $-\text{OH}$ and $-\text{O}^-$, and the acid strength of surface hydroxyls depends on the nature of the titania surface [17]. The positive and negative zeta potentials correspond to excess $-\text{OH}_2^+$ and $-\text{O}^-$ in average, respectively, and pH at which zeta potential is zero, i.e., point of zero charge (PZC), represents the pH giving the same number of $-\text{OH}_2^+$ and $-\text{O}^-$ on the surface. The difference in PZC in Fig. 3 suggests that the average acid strength of surface hydroxyls is in the order of OAT > P25 > DAT. Taking into account the preferential exposing facets of OAT and DAT, acid strength of hydroxyls on {101} facets is higher than that of hydroxyls on {001}. Such a difference in the surface charge may have an influence on the photocatalytic activity, e.g., through aggregation of particles in suspension to result in change in photoabsorption or enhancement/retardation of charge trappings and adsorption of substrates on

the surface. Studies on the relation of zeta potential with defect density are also in progress.

3.3 Photocatalytic Activity

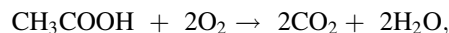
Table 2 shows the results of photocatalytic activity tests. In general, DAT exhibited photocatalytic activities higher than or comparable to those of P25 in all tested reaction systems, while OAT showed a relatively high level of activity in the photocatalytic oxidative decomposition of acetic acid but were less active for the other reactions.

Figure 4 shows the time-course curves of photocatalytic O_2 evolution from an aqueous solution of silver sulfate with suspended titania particles; the poor photocatalytic activity of OAT is clearly shown. For all samples, stoichiometric deposition of silver metal according to the equation

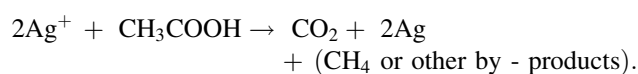


with molar amount four-times larger than that of O_2 , was observed (Fig. 4). It has been reported that the rate of this O_2 evolution depends remarkably on the amount of Ag^+ adsorbed on the surface of photocatalysts in the dark [17, 18] and it is expected, therefore, that the amount of Ag^+ adsorbed on OAT is insufficient to induce photocatalytic reaction. However, as shown in Table 1, the amount of adsorbed Ag^+ on OAT was not so small compared to the amounts adsorbed on DAT and P25, and surface density of adsorbed Ag^+ was almost the same regardless of the kind of titania particles. These results suggest that there is another reason for the lower level of photocatalytic activity of OAT in the silver sulfate solution. An additional activity test was performed to determine the reason.

Figure 5 shows the activities of several titania samples, including OAT, DAT and P25, for oxidative decomposition of acetic acid using O_2 in air or Ag^+ as an electron acceptor, i.e., an electron scavenger. Stoichiometry of the former reaction has been proved to be mineralization [19] as follows,



while that of the latter has not been established. Since methane was also liberated (e.g., ca. 10 μmol with DAT and P25 for 80-min irradiation) and the molar ratio of products, carbon dioxide and deposited silver, was approximately 2 for representative samples, OAT, DAT and P25 as indicated by Fig. 6, partial oxidation of acetic acid might occur as



Consequently, careful discussion is necessary for comparison of the rates of photocatalytic carbon dioxide liberation with O_2 and Ag^+ shown in Fig. 5. However, it is

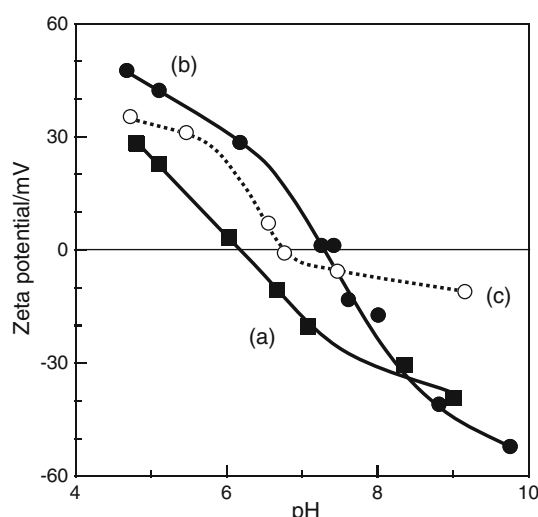


Fig. 3 Zeta-potential as a function of pH of suspensions of (a) OAT, (b) DAT and (c) P25 particles

Table 2 Photocatalytic activities of octahedral (OAT) and decahedral (DAT) single-crystalline anatase titania particles and a reference titania sample, Degussa P25

Sample ^a	Methanol dehydrogenation ^b ($\mu\text{mol h}^{-1}$)	Decomposition of acetic acid ^c ($\mu\text{mol h}^{-1}$)	O_2 evolution ^d ($\mu\text{mol h}^{-1}$)
OAT	229(28%) ^e	32(80%) ^e	2(11%) ^e
DAT	994(122%) ^e	48(120%) ^e	17(89%) ^e
P25	815	40	19

^a A 50-mg portion of each sample was used as a photocatalyst

^b Steady state rate of H_2 evolution from a deaerated aqueous solution of methanol (50 vol%; 5 mL) with in situ deposited platinum (2 wt%)

^c Steady state rate of carbon dioxide evolution from an aerated aqueous solution of acetic acid (5 vol%; 5 mL)

^d Initial rate of O_2 evolution from a deaerated aqueous solution of silver sulfate (25 mmol L⁻¹; 5 mL)

^e Figures in parentheses show photocatalytic activity ratio compared with that of P25 in each reaction

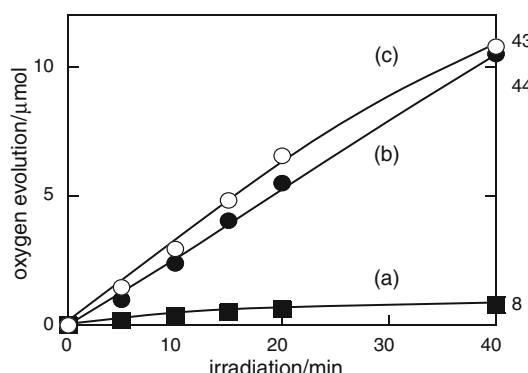


Fig. 4 Time-course curves of photocatalytic oxygen evolution from an aqueous silver sulfate solution with suspended (a) OAT, (b) DAT and (c) Degussa P25 titania particles. Figures in the right show the amount of deposited silver in the unit of μmol

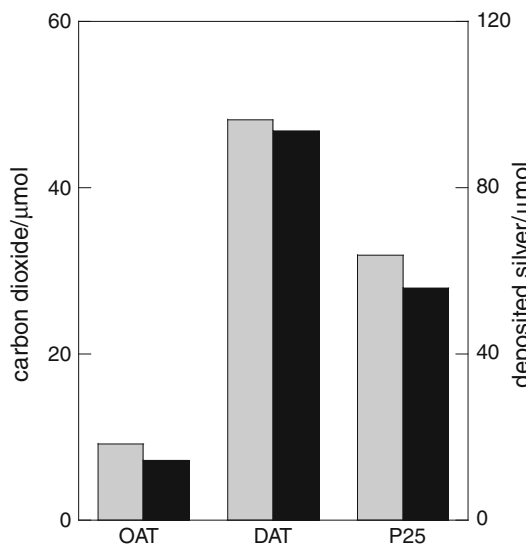


Fig. 6 Amount of photocatalytic liberation of carbon dioxide (left) and deposition of silver on the photocatalysts (right) from 5 vol% aqueous acetic acid under deaerated conditions in the presence of silver ions (250 μmol) (right) after 100-h (OAT) and 80-h (DAT and P25) photoirradiation

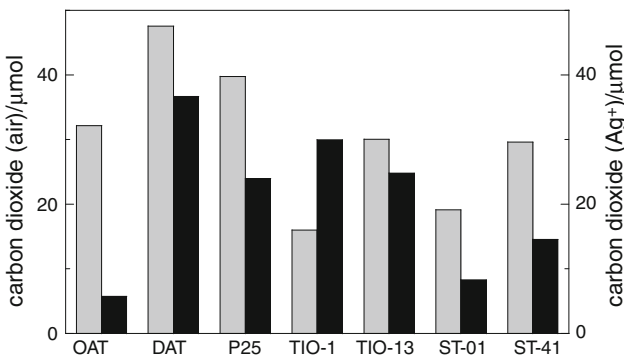


Fig. 5 Amount of photocatalytic liberation of carbon dioxide from 5 vol% aqueous acetic acid under aerated conditions (left) and under deaerated conditions in the presence of silver ions (250 μmol) (right) after 1-h photoirradiation. TIO-1, TIO-13, ST-01 and ST-41 are anatase powders with specific surface areas of 73, 65, 327 and 11 $\text{m}^2 \text{ g}^{-1}$, respectively

evident that the ratio of activity by changing the electron acceptor from O_2 to Ag^+ for OAT, ca. 20%, is exceptionally small compared with those for the other titanias; even ST-01 and ST-41 (Ishihara Sangyo) showed ca. 50% ratio (An exception, TIO-1, showing higher rate when Ag^+

was used may be due to reported contaminated sulfate anion on its surface to promote Ag^+ adsorption.).

These facts as well as the lower level of photocatalytic activity for O_2 evolution suggest that OAT is weak for reduction of Ag^+ by photoexcited electrons, while DAT and P25 exhibit all-round photocatalytic activities. The activity of OAT comparable to that of P25 in the presence of O_2 has also been shown: the photocatalytic activity of OAT for decomposition of methanol under aerated conditions was almost the same as that for decomposition of acetic acid under aerated conditions [8].

Results of SEM observation of deposited silver on OAT and DAT are shown in Fig. 7. Silver particles, with sizes of a few nanometers, were deposited on both samples. Although the rate of photocatalytic deposition was slow on

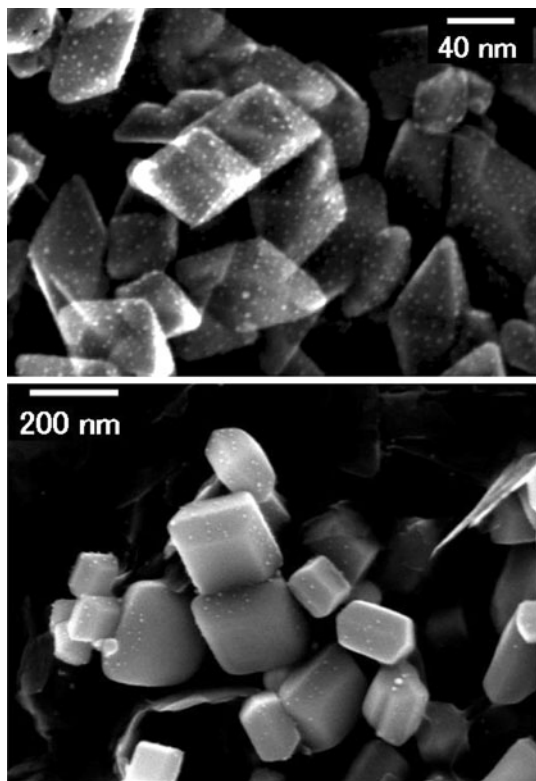


Fig. 7 SEM images of silver-photodeposited OAT (*upper*) and DAT (*lower*) particles photoirradiated in deaerated aqueous silver sulfate solutions for 80 and 40 min, respectively

OAT, the deposition seemed to proceed uniformly on its {101} facets. On the other hand, deposition on DAT, exposing {101} and {001} facets, occurred selectively on its {101} facets; no silver deposits could be found on {001} facets. Similar selective deposition of platinum particles has been reported for micrometer-scale decahedral anatase particles and was attributed to possible separation of reaction sites for reduction and oxidation: reduction by photoexcited electrons and oxidation by positive holes occur on {101} and {001} facets, respectively [20, 21]. This hypothesis seems consistent with the present observation of selective deposition of silver on {101} facets of DAT. However, the hypothesis seems too simplified to interpret the comparable photocatalytic activity of OAT exposing only {101} facets for decomposition of acetic acid in aerated suspensions. In this case, {101} facets must play roles of both oxidation and reduction sites.

3.4 Effect of Physical Properties on Photocatalytic Activity

It is reasonable to assume that photocatalytic activities are governed by physical and structural properties of a photocatalyst, and it is believed that there is correlation between photocatalytic activities and properties. At the

same time, it is also evident that the physical and structural properties are related to each other and it is practically impossible to change only one property without changing the others. This can be understood by remembering, e.g., that rutile titania powders are generally prepared by heating at a high temperature to give large particle size, small specific surface area or high crystallinity compared with those of anatase powders. Thus, it is difficult to determine the effect of crystal morphology, octahedral or decahedral, on their photocatalytic activities reported here.

We have recently reported the results of statistical analyses of photocatalytic activities and physical and structural properties of 35 commercial titania powders to find the predominant property (properties) determining the activity of a given reaction system [11]. It has been suggested that the reactions of O₂ and H₂ evolution under deaerated conditions, also employed in the present study, proceed preferably over titania photocatalysts of lower defect density, as is expected, while decomposition of acetic acid in aerated suspensions is promoted by higher defect density, presumably due to enhanced trapping of photoexcited electrons and their transfer to surface-adsorbed O₂. These suggestions at least qualitatively explain the present results shown in Table 2; OAT possessing a high defect density can exhibit comparable activity for acetic-acid decomposition, while its activity is relatively low for O₂ and H₂ evolution mainly due to its high defect density promoting recombination of photogenerated carriers. The reason for the characteristic higher defect density on the surface of OAT, whether it is intrinsically related to the structural properties of {101} facets, is not clear at present, as discussed in the preceding section. Photocatalytic activity of DAT better than or comparable to that of P25 in all the tested reactions might be due to the well-balanced physical and structural properties, but it is also not clear whether the crystal morphology has any influence on the properties.

4 Conclusions

Photocatalytic activities of OAT and DAT were examined and compared with those of Degussa P25 in several reaction systems. Both OAT and DAT exhibited activity levels higher than or comparable to that of P25 for oxidative decomposition of acetic acid in aerated aqueous solutions. DAT was also active for dehydrogenation of methanol and O₂ evolution under deaerated conditions, while OAT showed rather poor activity compared with that of P25 for these deaerated systems, suggesting that the relatively high density of crystal defects of OAT is beneficial for photocatalytic reactions, including reduction of O₂ by photoexcited electrons, and that the mechanism of reduction of

protons and Ag^+ is different from that of O_2 reduction. On the other hand, the observed all-round photocatalytic activity of DAT might be due to the possible good balance of physical and structural properties: moderate size of particles, specific surface area and defect density. Thus, the observed trends in photocatalytic activities of OAT and DAT could be explained, at least qualitatively, by conventional physical and structural properties. Further studies are therefore needed to draw conclusions regarding the presence of intrinsic effect of crystal morphology such as separation of redox sites and/or enhanced charge trappings, and research works along this line are now in progress.

Acknowledgments This work was partly supported by Project to Create Photocatalyst Industry for Recycling-oriented Society supported by NEDO, New Energy and Industrial Technology Development Organization. The authors thank Professor Tatsuya Tsukuda (Catalysis Research Center, Hokkaido University) for the permission to use of a zeta-potential analyzer. STEM analyses of samples were supported by Hokkaido Innovation through Nanotechnology Support (HINTS) of the Ministry of Education, Science, Culture and Sports of Japan.

References

1. Kaneko M, Okura I (2002) Photocatalysis: science and technology. Kodansha-Springer, Tokyo
2. Fujishima A, Zhang X, Tryk DA (2008) *Surf Sci Rep* 63:515
3. Yan X, Ohno T, Nishijima K, Abe R, Ohtani B (2006) *Chem Phys Lett* 429:606 (and references therein)
4. Amano F, Abe R, Ohtani B (2008) *Trans Mater Res Soc Jpn* 33:173 (and references therein)
5. Tian Y, Tatsuma T (2005) *J Am Chem Soc* 127:7632
6. Kowalska E, Abe R and Ohtani B (2009) *Chem Commun* 241
7. Irie H, Miura S, Nakamura R, Hashimoto K (2008) *Chem Lett* 37:252
8. Amano F, Yasumoto T, Prieto-Mahaney OO, Uchida S, Shibayama T, Ohtani B (2009) *Chem Commun* 2311
9. Amano F, Prieto-Mahaney OO, Terada Y, Yasumoto T, Shibayama T, Ohtani B (2009) *Chem Mater* 21:2601
10. Jpn. Patent (2005) P2005-162584A
11. Prieto-Mahaney OO, Murakami N, Abe R, Ohtani B (2009) *Chem Lett* 38:238
12. Murakami N, Prieto-Mahaney OO, Abe R, Torimoto T, Ohtani B (2007) *J Phys Chem C* 111:11927
13. Lazzari M, Vittadini A, Selloni A (2001) *Phys Rev B* 63:155409
14. Diebold U, Ruzicka N, Herman GS, Selloni A (2003) *Catal Today* 85:93
15. Abe R, Kusano D, Prieto-Mahaney OO, Amano F, Ohtani B *Langmuir* (to be submitted)
16. Ikeda S, Sugiyama N, Murakami S-Y, Kominami H, Kera Y, Noguchi H, Uosaki K, Torimoto T, Ohtani B (2003) *Phys Chem Chem Phys* 5:778
17. Ohtani B, Okugawa Y, Nishimoto S-I, Kagiya T (1987) *J Phys Chem* 91:3550
18. Nishimoto S-I, Ohtani B, Kajiwara H, Kagiya T (1983) *J Chem Soc, Faraday Trans* 179:2685
19. Kominami H, Kato J-I, Kohno M, Kera Y, Ohtani B (1996) *Chem Lett* 25:1051
20. Ohno T, Sarukawa K, Matsumura M (2002) *New J Chem* 26:1167
21. Taguchi T, Saito Y, Sarukawa K, Ohno T, Matsumura M (2003) *New J Chem* 27:1304